



Time invariant analysis of epidemics with EpiCompare

Shannon K. Gallagher

Biostatistics Research Branch
National Institute of Allergy
and Infectious Diseases

Benjamin LeRoy

Dept. of Statistics & Data Science
Carnegie Mellon University

Abstract

We present **EpiCompare**, an R package that supplements and enhances current infectious disease analysis pipelines and encourages comparisons across models and epidemics. A major contribution of this work is the set of novel *time-invariant* tools for model and epidemic comparisons - including time-invariant prediction bands. **EpiCompare** embraces R's *tidy* coding style to make adoption of the package easier and analysis faster. This paper provides an overview of both the tools in and intuition behind **EpiCompare** and a thorough demonstrating of the tools through a detailed example of a full data analysis pipeline.

Keywords: keywords, not capitalized, Java.

1. Introduction

The recent (and on-going) COVID-19 global pandemic has galvanized public interest in understanding more about infectious disease modeling and has highlighted the usefulness of research in the area of infectious disease epidemiology. Infectious diseases inflict enormous burdens on the world: millions of lives lost and trillions of dollars spent yearly. Infectious disease models typically attempt to do one or more of the following: 1) predict the spread of current and future epidemics (e.g. flu prediction [Biggerstaff *et al.* 2016](#)), 2) analyze past and current epidemics to increase scientific knowledge (e.g. historical measles outbreaks [Neal and Roberts 2004](#)), and 3) forecast or project epidemic scenarios under pre-specified parameters (e.g. [Ferguson *et al.* 2020](#)). At the same time, descriptive statistics and visualizations from universities, many branches and levels of government, and news organizations are an important first step of the process [as has been seen in the current COVID-19 epidemic](#) ([Dong *et al.*](#)

2020; CDC 2021; The Washington Post 2021).¹

With the many visualization and exploratory tools, models and modeling paradigms, and reviews and comparisons in the literature and through the MIDAS (Models of Infectious Disease Agent Study) network (MIDAS Network 2021), this field has a lot of devices to aid an individual practitioner decide the correct approach. For example, R packages such as **surveillance**, **EpiModel**, and **pomp** have all made significant steps in standardizing the flow of the data analysis pipeline for epidemic modeling through digitizing data sets, making accessible statistical models, and providing a plethora of educational material for both coding novices and experts alike (Meyer *et al.* 2017; Jenness *et al.* 2018; King *et al.* 2016).

At the same time, analysis packages often only address a specific portion of the analysis pipeline, ~~for instance focusing on certain types of models. These modeling tools, which~~ usually require learning package-specific syntax, and often don't provide easy ways to compare and assess their models on new data. Moreover, exploring, ~~and modeling and comparing~~ epidemics require transforming and *tidying* data in different ways. To fill these gaps, we present our R package **EpiCompare**. Our package's primary focus is to aid and advance research in the area of comparison and assessment of epidemic and epidemiological models. In Figure 1, we illustrate the data analysis pipeline of infectious diseases as 1) data pre-processing, 2) exploratory data analysis (EDA), 3) modeling and simulating, 4) post-processing, and 5) comparison and assessment; where each previous part of the pipeline influences the next. **EpiCompare** provides tools to aids practitioners in all areas of this pipeline.

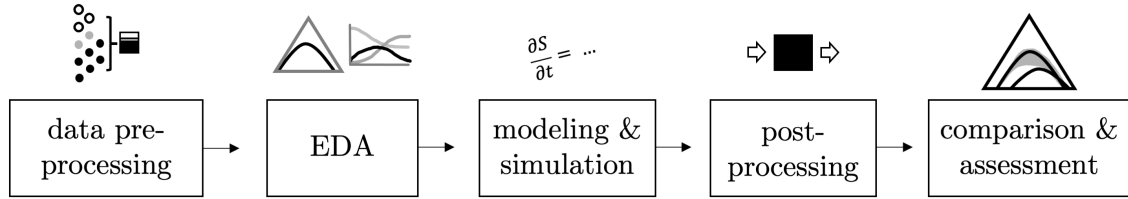


Figure 1: An idealized epidemiological data analysis pipeline.

EpiCompare also emphasizes the value of analyzing epidemics in a *time-invariant* way. Epidemics, despite by definition being a process that evolves over time, often need to be compared in a way not constrained to initial times or time scales to understand the processes at play. Time-invariant analysis can also make it easier to compare state-space models in a more global, holistic fashion. ~~Moreover, m~~ Many current time-dependent comparison tools for state-space models (e.g. SIR models) ~~highlight~~ examine the proportion of individuals in each state (at a given time) in a piece-wise / marginal fashion. ~~These This~~ approaches may reduce the amount of connections that can be seen, similar to projections of a multidimensional distribution onto a single axis at a time. Tools in **EpiCompare** give the user the ability to extend their toolkit to evaluate epidemics within a time-invariant lens. The goal of **EpiCompare** is not to supplant existing infectious disease modeling tools and software but, rather, is a concerted effort

¹[Ben says: probably should have a conclusion sentence here - seems to end abruptly. *This is less so the case now.]

to create standard and fair comparisons among models developed for disease outbreaks and outbreak data.

This paper is broken up into the following sections; section 2 motivates and showcases tools of time-invariant analysis, section 3 presents an outline of how **EpiCompare** aids a practitioner in every step of the pipeline and section 4 provides a **thorough** demonstrating of the tools through a detailed example of a full data analysis pipeline.

2. Motivation and tools for time-invariant analysis

EpiCompare delivers *time-invariant* analysis by (1) taking a global, not marginal view of how epidemics move through populations and (2) by treating full epidemics as filamental trajectories² and not points produced by functions of time³ (this will be explained in Section ??). The following section aims to highlight the strengths of *time-invariance* and define the mathematical foundations that **EpiCompare**'s tools stand upon.

Mathematically, epidemics are complex objects. They can be hard to assess and compare to one another due to the differences in the diseases, the location where the outbreak occurs, how the affected population reacts, and the time related features (including start of the epidemic, speed of infection and more). Time-invariant analysis make different epidemics easier to compare by removing many time dependent aspects of an epidemic. Instead it focuses on the overall trajectory of an epidemic, emphasizing the number of lives affected.

2.1. Motivating time-invariance through R_0 ⁴

Time-invariance analysis, as it appears in **EpiCompare**, ~~can be seen as an attempt to escape~~ **bypasses** many difficulties **in** comparing different epidemics. With time-invariant analysis, comparing the decades-long outbreak of HIV in the US to a 10 day outbreak of norovirus on a cruise ship is still possible. Time-dependent problems can arise when estimating epidemiological parameters, including the reproduction number R_0 . **We will use R_0 to motivate the usefulness of time-invariant analysis in this section.**

R_0 is probably the most famous time-invariant numerical summary of an epidemic and is often associated with the Susceptible-Infectious-Recovered (SIR) model (?)⁵. R_0 is a one-number summary of a disease and is defined as the expected number of infections caused by a single infector who is added to a completely susceptible population (Anderson and May 1992). R_0 can be a difficult quantity to estimate and is typically sensitive to time-based parameters such as the beginning and end of an epidemic (Gallagher *et al.* 2020). [Ben says: Shannon could we expand on this difficulty / show it really is difficult with 1 more sentence? It might benefit from listing the difficulting in estimating a robust R_0 value (difficulties: time steps used, scale and "start" and final start, assumptions about population growth and underlying model fit).] To demonstrate the difficulty of discerning R_0 in a time-dependent analysis, we first introduce the Kermack and McKendrick (1927)'s SIR model. This model captures the transitions from one state to the next as a system of ordinary differential equations, where N is the total number of individuals, β is the rate of infection, and γ is the rate of recovery,

²[Ben says: Do we need a footnote explaining what this is more clearly?]

³[Shannon says: this notation needs to be cleaned up.]

⁴Is this still a relevant title for this section? Think about this header after the rewrite.

⁵[Shannon: correct CITation]

$$\begin{aligned}
S'(t) &= -\frac{\beta S(t)I(t)}{N} \\
I'(t) &= \frac{\beta S(t)I(t)}{N} - \gamma I(t) \\
R'(t) &= \gamma I(t).
\end{aligned} \tag{1}$$

From this model, $R_0 = \beta/\gamma$, aka the ratio of the infection rate compared to the recovery rate. Since β and γ are both rates, the ratio of the two, R_0 , is a time-invariant quantity. Once R_0 is estimated, practioners can infer important epidemic quantities such as the total number of infections or the percent of a population needed to be vaccinated to stop the sustained spread of an epidemic. Moreover, R_0 allows us to compare different diseases and different instances of outbreaks on the same scale.

2.2. ~~Visualizing~~ R_0

[Ben says: It's unclear to me why we have a subtitle here - isn't it just more motivation of time-invariant anlysis with R_0 ? Also, I feel like the story is weak here. The point is to leverage R_0 to show the value of time-invariant analysis - this seems a bit more like just discussing properties of R_0 . In the follow rewrite I use "[" and "]" to indicate that this is a section from your earlier draft.]

[Ben says: replacement of following paragraph: presentation rearranged to emphasis the figure first (when presenting the problem), and then discussing it.] Traditional *state* vs. *time* plots, like seen in Fig. 2, present information about epidemics in a time-dependent and piece-wise fashion, and make comparing different epidemic R_0 s impossible. In Fig. 2 we compare [two different epidemics that start in two populations of 1000 people with 10 individuals initially infected, but with different infection and recovery rates (see Eq. 1)]. More specifically, we've observed both epidemics for 15 days, with the first epidemic⁶ (in red) having parameters $\beta_1, \gamma_1 = (1, 2)$ and the second epidemic (in blue) having parameters $\beta_2, \gamma_2 = (2, 4)$. [At a glance, we may believe that Model epidemic 1 has a larger R_0 than Model epidemic 2 because the peak of infection occurs more quickly than in Model 2 (remember R_0 relates to the rate of infection). On the other hand, we may believe Model epidemic 2 has a larger R_0 because its unclear if the number of infections in that model epidemic has not yet peaked at time 15. Yet, both epidemics have the same R_0 of 2].

[Ben says: bring Fig. 2 here.]

[Ben says: this paragraph is replaced with the one above] With regards to traditional epidemic *state* vs. *time* plots, when ~~comparing~~ examining different epidemics their R_0 s are often impossible to compare. This can be seen in a basic example, where we have two different epidemics that start in two populations of 1000 people with 10 individuals initially infected, but with ~~different parameters~~ different infection and recovery rates (see Eq. 1). Specifically suppose that $\beta_1, \gamma_1 = (a, b)$ and $\beta_2, \gamma_2 = (ca, cb)$ where $a, b, c > 0$. Further suppose we observe both of these epidemics for 15 days. The epidemic trajectories are shown in the *state* vs. *time* plots in Figure 2. At a glance, we may ~~assume~~ believe that Model 1 has a larger R_0 than Model 2 because the peak of infection occurs more quickly than in Model 2. On the other hand, we

⁶In the plot it says model - probably want to say epidemic?

may ~~think~~ **believe** Model 2 has a larger R_0 because we may think the number of infections in that model has not yet peaked at time 15. Yet, both epidemics have the same R_0 of 2.

Introduce ternary plots here. The below paragraphs are mostly new

[Ben says: another rewrite of the paragraph below.] A time-invariant approach to visualizing epidemics, which will be described more below, provides a simple way to compare R_0 values of epidemics that are generated from the Kermack and McKendrick SIR model. In these visuals, we treat epidemics as *filamental trajectories*. A filamental trajectory can be mathematically viewed as a set of points in space that have an ordering, and that all points on the line between these order points are also contained in the geometric object. For a SIR epidemic, we can represent the associated filamental trajectory ψ as

$$\psi = \{(S(t), I(t), R(t)) : S, I, R \geq 0, S + I + R = N\}_{t \in [0, T]},$$

where the an mapping $\xi : t \rightarrow \mathbb{R}$ that is monotonically increasing would not change the definition of ψ , i.e. $\psi_\xi = \psi$ where :

$$\psi_\xi = \{(S(\xi(t)), I(\xi(t)), R(\xi(t))) : S, I, R \geq 0, S + I + R = N\}_{t \in [0, T]}.$$

[Since the number in each state is non-negative and the sum over the three states for a given time point sums to N , then ~~all points in ψ will lay in a 2d triangular plane, i.e. a ternary plot~~ two-dimensional triangular plane in the three-dimensional space, which can be visualized in a two-dimensional ternary plot. As a result, we can visualize the global trajectory of an epidemic in a single ternary plot ~~2d plot and ultimately R_0~~ . **[Shannon says: Show pic here?]**⁷

[Ben says: this paragraph was replaced with the paragraph above] ~~However, time-invariant centric analysis allows us to visualize R_0 for the Kermack and McKendrick SIR model. We call the epidemic trajectory of number of individuals in each state a *filament*. Mathematically, a filament ψ for the SIR model ψ this is the set of points of the number in each state for each time point,~~

$$\psi = \{(S(t), I(t), R(t)) : S, I, R \geq 0, S + I + R = N\}_{t=0:T}.$$

~~Since the number in each state is non-negative and the sum over the three states for a given time point sums to N , then ψ will lay in a 2d triangular plane, i.e. a ternary plot. As a result, we can visualize the global trajectory of an epidemic in a single 2d plot and ultimately R_0 . Show pic here?~~

[This section could be a bit less wordy. But generally good.] We visualize the two epidemics in a global, ternary view in Figure 3. Without getting into too much detail of the intricacies of this plot, we immediately see the points of the two filaments ψ seem to form the same trajectory. Now, it is much clearer that **Model epidemic 2** is following the same trajectory as **Model epidemic 1** but is not as far along in the infection process. We can see there is something fundamentally linking these two different epidemics, and this fundamental link turns out to be R_0 .

We can show this mathematically. ~~if we~~ **Let** our two epidemics be presented as $\{(S_1(t), I_1(t), R_1(t))\}_{t \geq 0}$, $\{(S_2(s), I_2(s), R_2(s))\}_{s \geq 0}$ respectively.⁸ As with the example, assume both models have the same initial values $(S(0), I(0), R(0))$, and let $R_0 = \frac{\beta_1}{\gamma_1} = \frac{\beta_2}{\gamma_2}$ where β_i and γ_i are the average

⁷Which?

⁸**[Ben says: Originally this was a sentence fragment.]**

infection rate and recovery rate, respectively, for SIR model $i = 1, 2$. And define $a > 0$ to be the relative scalar such that $\beta_2 = a\beta_1$ if and only if $\gamma_2 = a\gamma_1$.

Theorem 1. *Let there be two SIR models as described above. Then for all $t > 0$ there exists an $s > 0$ such that $(S_1(t), I_1(t), R_1(t)) = (S_2(s), I_2(s), R_2(s))$. Moreover, $s = \frac{1}{a}t$.*

The proof of Theorem 1 relies on a fairly recent result from [Harko et al. \(2014\)](#) and is shown in detail in Proof 4.1. The consequence of Theorem 1 is that for two SIR models that have the same initial percent of individuals in each state and R_0 then for every point on the epidemic path of the first SIR model ~~is also~~ can be mapped to a point on the epidemic path of the second SIR model. [We've changed how we describe these two objects when they are related to the theorem - is that desirable?]

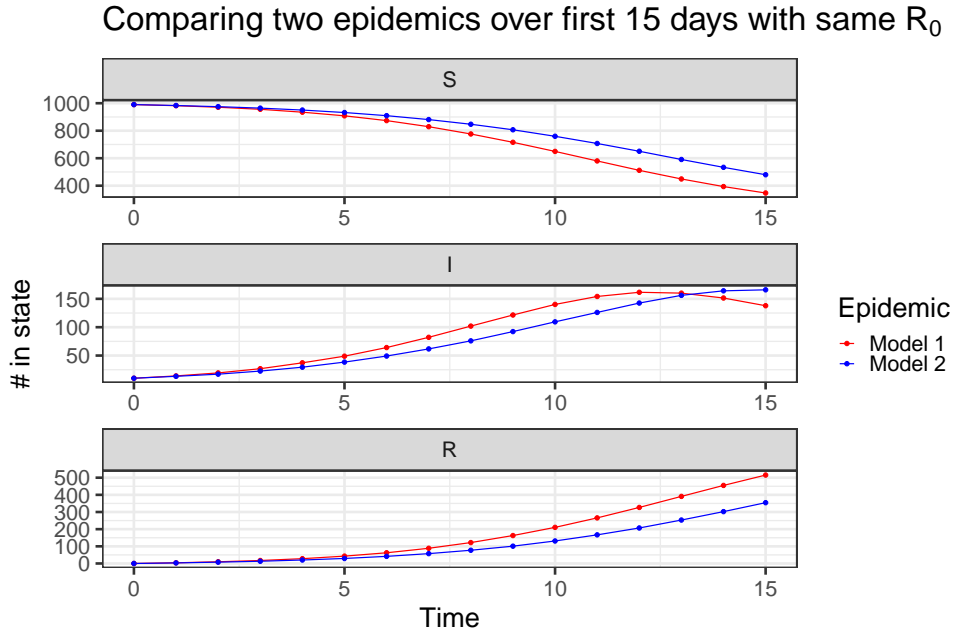


Figure 2: Example of two epidemics with different β and γ parameters but the same initial reproduction number $R_0 = 2$. Both plots are generated from models with $N = 1000$ individuals with $S(0) = 990$ and $I(0) = 10$.

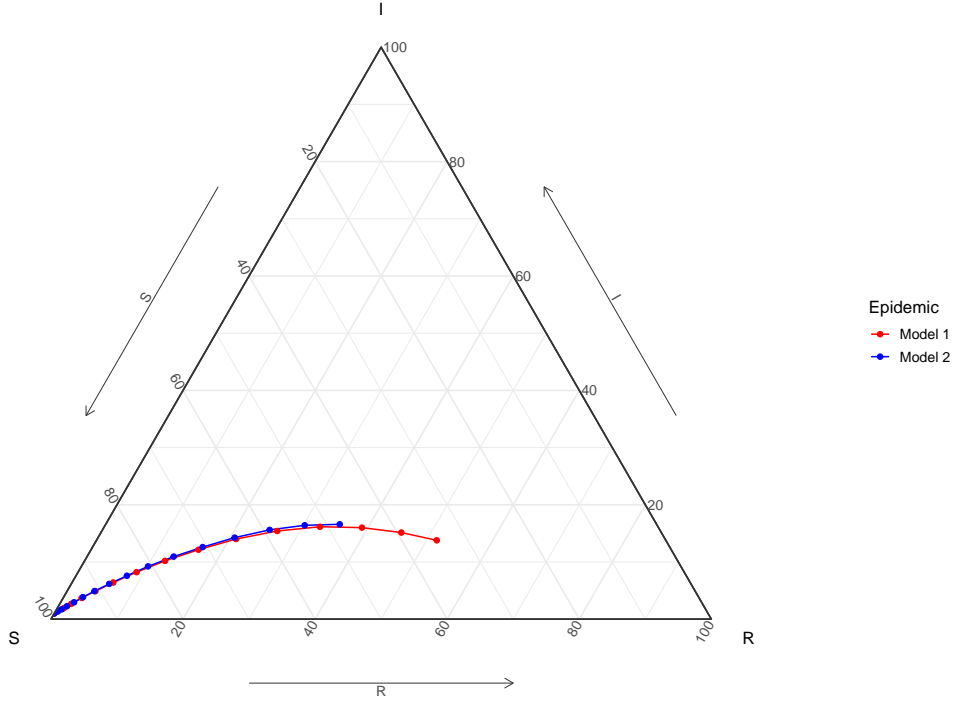


Figure 3: Example of two epidemics with different β and γ parameters but the same initial reproduction number $R_0 = 2$. Both plots are generated from models with $N = 1000$ individuals with $S(0) = 990$ and $I(0) = 10$. These are plotted in the time-invariant view, where we can see the number of susceptible, infectious, and recovered.

2.3. Time-invariant analysis Beyond R_0 and Kermack’s and McKendrick SIR Models⁹

Through the R_0 example, we see that treating epidemics like a filamental trajectories embedded in a lower dimensional space allows us to better compare the overall structure of the epidemic and see how the population was directly impacted. In this section we will present time-invariant tools that can be useful even when the underlying generative model for the epidemic is unknown. We will also present how this tools can be used when the epidemics have more than 3 states. trajectories, we propose that time-invariant tools can help compare them in smart ways, and that these ideas can extend past the CITE kermack1927 model and to epidemics with more states.

New paragraph Viewing epidemics as filamental trajectories provide a lot new ways to compare and examine epidemics in a time-invariant manner. For epidemics that have “played” themselves out, one way to represent their filamental trajectories to avoid impacts of temporal structure is to define them as a sequence of points their trajectory with equi-distance between each point. This also creates a natural distance between this type of representation between epidemics, specifically:

$$d_{\text{equi-distance}}(\psi_1, \psi_2) = \int_{s \in [0,1]} (\psi'_1(s) - \psi'_2(s))^2 ds$$

⁹Probably will need to change this title...

where $\psi'_i(s)$ the point along ψ_1 that is s fraction of $|\psi_1|$ distance away from the start of ψ_i . This distance is naturally time-invariant, and can be plugged into multiple distance-based assessment tools to examine the overall extremeness of points, including psuedo-density estimators and depth/local depth functions (for examples see [Ciollaro *et al.* 2016](#); [Geenens and Nieto-Reyes 2017](#)). This can be very useful when comparing between a set of simulation epidemics and the true epidemic, and does not constrain the number of states of the model, though we recommend projecting the points into the unit simplex¹⁰ (by making all values the proportion of the population in the given state).

New paragraph: If the set of epidemics that one is examining have only gone through a single cycle of the outbreak (before the population of individuals have become susceptible again), then additional time-invariant tools, including prediction regions can be leveraged. In these settings we go a step farther and treat epidemics more like geometric filaments than filamental trajectories. In **EpiCompare** we create prediction regions that contain a the top $(1 - \alpha)$ proportion of simulated curves by defining geometric regions defined by the union of small filaments around the subset of simulations (subset by measures like the above psuedo-density estimates or depth estimates). These regions look at where in the state-space we expect the epidemic to traverse, and we can compare prediction regions defined by different models using the Hausdorff distance as well as examining how well the truth epidemic matches the simulations by examining if the epidemic’s trajectory lies within the prediction region. All these geometric structures and distances notations apply to epidemics with any number of states, and at the end of Section 3 we also highlight how these prediction regions can aid in visual comparisons for epidemics with 3 states (like the SIR models).

[Ben says: Old recommendations: to be continued - (1) highlight filamental view of the epidemics through their simplex space (2) describe distances that could compare different epidemics with this mindset. Also motivate uncertainty for epidemics now that we have a filamental view (3) emphasis that this idea should extend to higher dimensions (4) present the idea that one could also compare bands together.]

3. Overview of EpiCompare

In this section, we present the tools implemented in **EpiCompare** and explain how they aid in the data analysis pipeline. In Fig. 4, we illustrate how our package’s functions fit into the data analysis pipeline introduced in Fig. 1. All front-facing functions are aimed to be as user-friendly as possible. We also focus on providing the user “tidyverse” style functions, that encourage piping and also follow clear verb naming schemes ([Wickham *et al.* 2019](#)). Although users can typically incorporate **EpiCompare** into any step in the data analysis process, there are two primary points of entry. The first point of entry is the very beginning with pre-processing and visualizing raw data, and the second point of entry is after modeling and simulation. Figure 4 captures these different paths, and we will highlight¹¹ both approaches and how to leverage **EpiCompare** in the subsections below.

Data Pre-processing

The first step of most data analysis is cleaning the data so it can be explored. There are multiple ways to collect epidemiological data. Sometimes individual records are collected,

¹⁰I’m not sure we’ve talked about this before...

¹¹[Ben says: we need to make sure we actually do highlight]

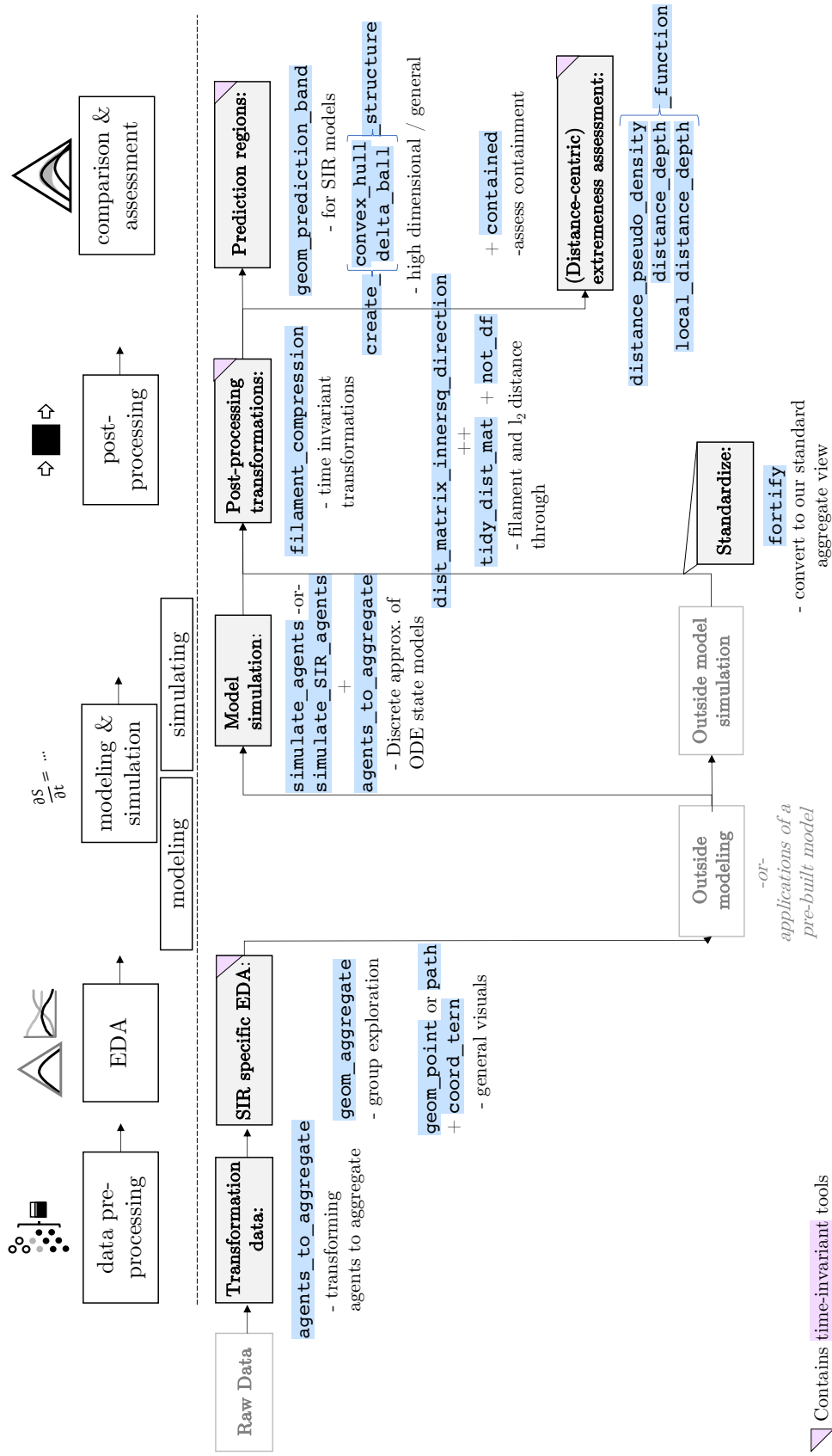


Figure 4: How EpiCompare supplements and aids in the epidemiological data analysis pipeline.

with times of different states of the epidemic (infection, recovery, etc.) as well as individual information like network structure, location, and sub-population information. Other data collections focus on aggregate counts of individuals in each epidemic state. In fact, usually only the number of new infections at each time step (e.g. weekly case counts) is observed. Compartment totals (amounts of individuals in each state) are then imputed from those case counts along with other information about the disease and the population of interest. In **EpiCompare**, we focus on understanding the overall impact of an outbreak at the aggregate/population level, which allows for examination of overall trends of an epidemic more easily.

In order to help the practitioner examine epidemics from an aggregate/ population lens, we provide a function called `agents_to_aggregate`. This function transforms data about individual/agents' initial entry into each state (e.g. start of infection, start of recovery, etc.) to an aggregate view of how many individuals were in a state at a given time. There are often situations where grouping agents into subpopulations (e.g. subpopulations defined by age or sex) can highlight different aggregate level trends. For example, research by [Rvachev and Longini \(1985\)](#); [Anderson and May \(1992\)](#); [Worby et al. \(2015\)](#) develop state-based models that account for subpopulations. In **EpiCompare**, we facilitate subpopulation analysis by combining `dplyr::group_by` and `agent_to_aggregate` to provide aggregation at a group level.

The `agents_to_aggregate` function is flexible and can deal with a wide range of information about each individual. It can, theoretically, account for infinitely many states. This functionality allows the practitioner to aggregate information relative to the standard states (e.g. "Susceptible", "Infectious", and "Recovered") as well as add states (e.g. "Exposed", "Immune", "Hospitalized") (CITE¹²). Additionally, `agents_to_aggregate` also permits indicators for death/exit and birth/entry dates. Overall, the function `agents_to_aggregate()` is a powerful tool for pre-processing data.

EDA

With raw data, "getting to know" our data currently means figuring out good combinations of visualizations, numerical summaries and subsets. An expert coder has many ways to successfully explore the data in an aggregate lens using `agents_to_aggregate`. **EpiCompare** also includes tools to rapidly explore data that has three epidemic states. Building on the tools in **ggplot2** and **ggtern**, our `geom_aggregate` provides a rapid way to explore different subpopulations' experience of an epidemic by combining the ideas behind `agents_to_aggregate` for three-state models to examine subpopulation trajectories in a 3d simplex space ([Wickham 2016](#); [Hamilton and Ferry 2018](#)). [\[Shannon says: come back - think about spaces and trajectories?\]](#)¹³ Visualization tools for three-state models were developed because (1) SIR models are some of the most common and basic epidemic state-based models and (2) our simplex representation of these epidemics emphasizes a "time-invariance" representation of the data (for a refresher see Section 2). [\[Shannon says: make sure SIR is defined before.\]](#)

Model Fitting and Simulations

[\[Ben says: think about this section and if it highlights that we can bring in outside models...\]](#)
 After getting a good sense of what a past or current epidemic looks like through EDA, the next step is often model fitting and/or simulations. In this step, and the next step

¹²[Ben says: this was originally to back up the claim that SIR is the "standard" states - now we might need to have a paper that says that SIR is the standard states and also suggests other states...]

¹³[Ben says: what does this note mean?]

(post-processing), we discuss how to include practioners' use of tools to create models and simulations that exist outside of **EpiCompare**. This package does not focus on fitting a model to data, we do provide some flexible functions for simulation of basic discrete-time epidemic-state models. After estimating or predicting transition rates between states, these functions produce individual level ~~simulationsinformation~~ and can be ~~naturally~~ combined with `agents_to_aggregate()` to view these simulations through an aggregate lens. The function `simulate_SIR_agents()` simulates an SIR epidemic with user inputs for the number of simulations, the initial number in each state, the infection and recovery parameters (β, γ), and the total number of discrete time steps. This function allows for easy access to SIR model analysis and comparison. Beyond SIR models, the function `simulate_agents()` takes as input a user-specified transition matrix and other epidemic parameters to allow the user to create simulations of an outbreak for *any* number of states and any number of transitions among them. This flexibility in states can be used to also reflect group-based dynamics. This allows for users to explore the space of models in an intuitive way without getting bogged down by too much mathematical detail. For consistency, we have made output from `simulate_agents()` and `simulate_SIR_agents()` compatible with `agents_to_aggregate()` so aggregate information may easily be accessed.

Post-processing

[Ben says: I think we should remind the reader that we care more about simulations, in order to compare fitted models between themselves and the true epidemics.]

[Ben says: this replaces the first paragraph below]

If the practitioner wishes to compare between models and with their true epidemics, one needs to process their models and simulations. In general, [post-processing of modeling and simulation consists of making summary statistics, plots, tables, and other ways to disseminate information to the public.] The summaries can be very complex, and a[s] result, a number of epidemic modeling **R** packages return a special class, specific to their modeling. The special classes often contain a plethora of information from residuals, model diagnostics, input parameters, and more. While incredibly useful, these special classes can be difficult for novice coders to navigate.]

[Ben says: replaced with above paragraph] Post-processing of modeling and simulation consists of making summary statistics, plots, tables, and other ways to disseminate information to the public. For example, comma separated value files (`.csv`) are a standard way to share information within tables. However, model output is often far more complicated than what a traditional `.csv` would allow. Do we need three sentences about csvs? As a result, a number of epidemic modeling packages return a special class, specific to their modeling. The special classes often contain a plethora of information from residuals, model diagnostics, input parameters, and more. While incredibly useful, these special classes can be difficult for novice coders to navigate.

To this end, we have ~~provideadapted~~ a series of **fortify**-style ~~methodsfunctions~~¹⁴, called `fortify_aggregate()` which transform output from packages like **pomp** and **EpiModel** into tidy-styled data frames which contain information about the total number of individuals in each state at a given time, for a given simulation. These fortify functions have output that is consistent with that of `agents_to_aggregate()`.

[Ben says: new paragraph] To utilize simulations epidemics in later time-invariant analysis we

¹⁴[Ben says: Not tied to this change.]

also provide a function to convert temporally defined epidemics to filamental representations. Specifically, we provide the function `filament_compression` to convert simulation(s) to filaments as expressed by presenting the epidemic as a ordering of some common fixed number of points so that they are equally spaced along the original path in the proportional state space¹⁵.

Comparisons and Assessment

[This still needs to be worked on - just a reminder.]

Comparison and assessment of model fit or comparisons of one model to another model can be performed in a variety of ways including mean square error, AIC, plots, and more. Perhaps the most useful tool **EpiCompare** has to offer to the expert, for comparison and assessment of models, is in its post-processing tools which create a standard output. It is then a matter of writing a script or function made for that standard output to assess the results from multiple models in the way the user desires¹⁶.

However, for those who like more concrete tools, **EpiCompare** offers functions to compare prediction regions to one another including `geom_prediction_band()` (which plots the region), and `create_{convex_hull,delta_ball}_structure()` (which returns the R output for the given structure), and `contained()` (which allows the user to determine if one set of points is contained in a prediction band). Additionally, we offer ways to determine if model outputs are compatible with one another, that is how extreme one output is to another. Ben says something about distance

4. A tour of EpiCompare

In this section, we highlight a number of the functionality available in **EpiCompare**. These functionality include data cleaning, visualization, simulation, and comparison, in accordance with the data analysis pipeline 1. We show a full data analysis from beginning to end that can be accomplished in a streamlined and standardized manner.

4.1. Data and exploratory analysis

We analyze an outbreak of measles in the town of Hagelloch, Germany from 1861-1862, a data set organized by Pfeilsticker (1863). The data was later made visible by Oesterle (1992) and made available in an R by Meyer *et al.* (2017). The Hagelloch data includes a rich set of features including household members, school level, household locations, date of first symptoms (prodromes), date of measles rash, and even the alleged infector. A subset of the data is shown in Table 1. Because of these rich features, this data set has been an ideal testing ground methodology in infectious disease epidemiology and is used in work by Neal and Roberts (2004); Britton *et al.* (2011); Groendyke *et al.* (2012); Becker *et al.* (2016).

With **EpiCompare**, we can easily obtain the empirical cumulative incidence function with respect to the measles rash appearance (variable ERU) with the following tidy-style function, `agents_to_aggregate`. The function `agents_to_aggregate` is a key component of **EpiCompare**, allowing the user to easily switch from an individual-level (i.e. an agent) view of a

¹⁵[Ben: this should be cleaned up.]

¹⁶[Ben says: Shannon, doesn't this below in the previous section?, I might drop this paragraph except for the introduction sentence - is it really true that the standardization is most valuable?]

Table 1: Subset of Hagelloch infection data. Features include the person ID, household ID (HH ID), age, sex, class level (Pre-K/1st/2nd), date of first symptoms, date of the appearance of the measles rash, and the alleged infector ID of the individual.

ID	HH ID	Name	Age	Sex	Class	Symp. Start	Rash Date	Infector ID
1	61	Mueller	7	female	1st class	1861-11-21	1861-11-25	45
2	61	Mueller	6	female	1st class	1861-11-23	1861-11-27	45
3	61	Mueller	4	female	preschool	1861-11-28	1861-12-02	172
4	62	Seibold	13	male	2nd class	1861-11-27	1861-11-28	180
5	63	Motzer	8	female	1st class	1861-11-22	1861-11-27	45
45	51	Goehring	7	male	1st class	1861-11-11	1861-11-13	184

disease to an aggregate level. For example, the below code shows how we can convert the agent data to a cumulative incidence of the measles rash, in order to see how the disease spread through the population over time. We can then compare the cumulative incidence of the rash to the cumulative incidence of the prodromes, i.e. the initial symptoms. We do this with the below code, and a part of the cumulative incidence data output are shown in Table 2. The argument `integer_time_expansion` indicates whether we should include all time points in the recorded range of the data or only when there is a change in the incidence.

```
R> cif_rash <- hagelloch_raw %>%
+   mutate(time_of_rash = as.numeric(ERU - min(PRO, na.rm = TRUE))) %>%
+   agents_to_aggregate(states = time_of_rash,
+                       integer_time_expansion = FALSE) %>%
+   mutate(type = "Rash")
```

Table 2: Turning the individual-level information from the Hagelloch data to an aggregate view of the cumulative incidence of the measles rash in the population over time.

Time	# Susceptible	# Total rash appearances
0	188	0
4	187	1
7	186	2
9	185	3
12	183	5

One question of interest is the duration between initial onset of prodromes or symptoms and the appearance of the measles rash. Since `agent_to_aggregate` outputs a tidy-style data frame, it is a simple task to plot the two sets of incidence curves on the same graph (Fig. 5).

```
R> cif_prodromes <- hagelloch_raw %>%
+   mutate(time_of_PRO = as.numeric(PRO - min(PRO, na.rm = TRUE))) %>%
+   agents_to_aggregate(states = time_of_PRO,
```

```

+               integer_time_expansion = FALSE) %>%
+   mutate(type = "Pro")

R> plot_df <- bind_rows(cif_rash, cif_prodrumes)
R>
R> ggplot(data = plot_df,
+   aes(x = t, y = X1, col = type)) +
+   geom_step() +
+   labs(title = "Cumulative incidence of measles appearance",
+     x = "Time (days relative to first prodrome appearance)",
+     y = "Cumulative incidence of event") +
+   coord_cartesian(xlim = c(0, 55)) +
+   scale_color_manual(values = c("blue", "red"))

```

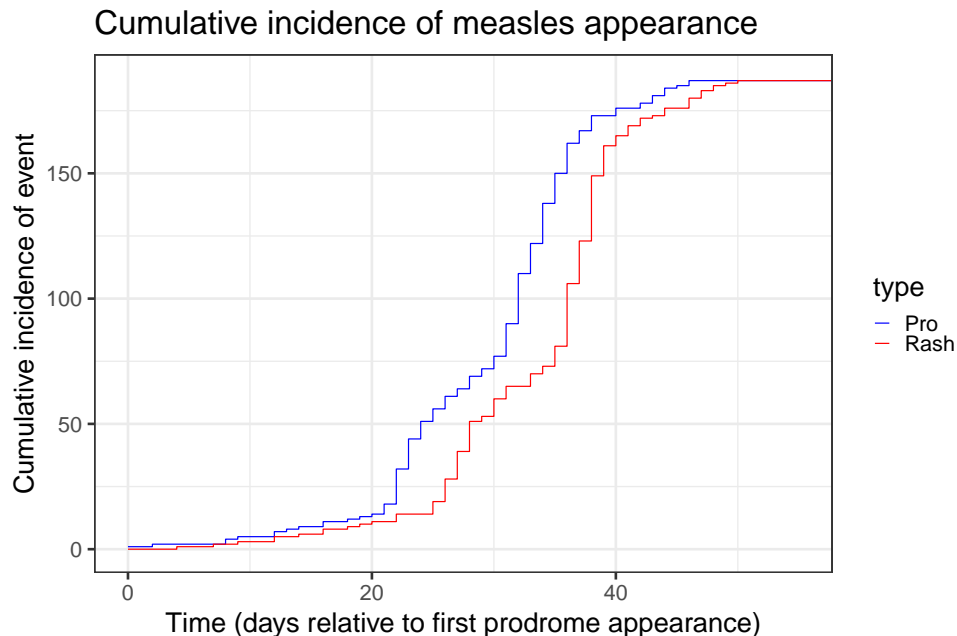


Figure 5: Empirical cumulative incidence functions of prodrome (symptom) onset and measles rash appearance. We see that there is approximately a constant lag between the two curves.

The real power of `agents_to_aggregate()` lies in its ability to aggregate over any number of pre-specified states. For example, the Hagelloch data sets contains two columns, `tI` and `tR`, the time of infection and recovery, respectively of each individual. We can then plot the SIR values through a time-invariant lens using `ggplot2` and `ggtern` functions (as shown in Fig. 6) or with our custom `geom`, `geom_aggregate`, which takes the raw agent data as input.

```

R> hagelloch_sir <- hagelloch_raw %>%
+   agents_to_aggregate(states = c(tI, tR),
+     min_max_time = c(0, 55)) %>%
+   rename(time = t, S = X0, I = X1, R = X2)

```

```

R>
R>
R> ggplot(hagelloch_sir, aes(x = S, y = I, z = R)) +
+   coord_tern() +
+   geom_path() +
+   labs(x = "S", y = "I", z = "R",
+         title = "Time invariant view of Hagelloch measles outbreak") +
+   theme_sir(base_size = 24)

```

Time invariant view of Hagelloch measles outbreak

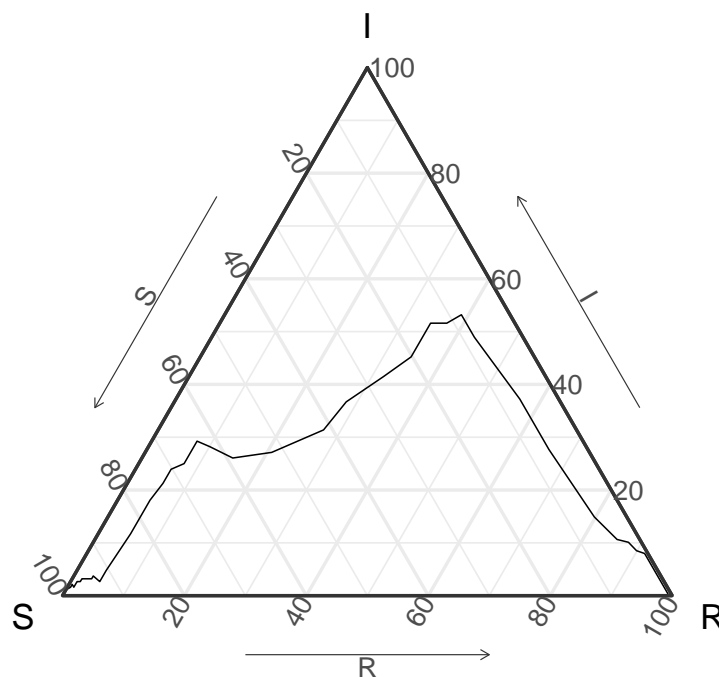


Figure 6: Time invariant view of the Hagelloch epidemic where we view the individuals in Susceptible, Infectious, or Recovered states. We see there are two peaks of infection (the vertical axis).

Moreover, we can look at the outbreaks of the disease by group within `agent_to_aggregate()` or `geom_aggregate()`. This allows us to examine differences among the different groups of individuals. For example, we show the time invariant outbreak by class level in Figure 7. Immediately, we see that time invariant infection curve is different for the pre-school class compared to the 1st class. In the 1st class, we see about 95% of the class become infected and less than 10% of them having recovered, which is indicative of a super-spreading event. This suspicion is further confirmed in that 26 of the 30 1st class students have been reportedly infected by the same individual.

```

R> hagelloch_raw %>%
+   ggplot(aes(y = tI, z = tR, color = CL)) +

```



```
+ geom_aggregate(size = 2) + coord_tern() +
+ labs(x = "S", y = "I", z = "R",
+       color = "Class") +
+ scale_color_brewer(palette = "Dark2") +
+ facet_wrap(~CL)
```

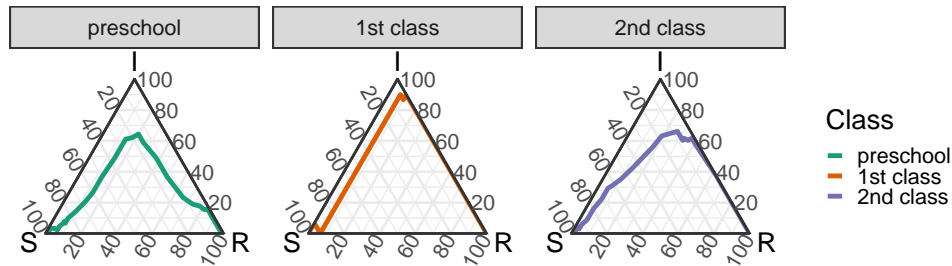


Figure 7: Time invariant outbreak curves for the three class groups. The pre-school class has a distinct peak of infection whereas the peak infection point for the other two classes are less well defined.

Along with multiple epidemic states, the function `agents_to_aggregate` can also be extended to populations with vital dynamics (e.g. birth and death) and examples of this are shown in the package vignette. In summary, `agents_to_aggregate()` is a multi-purpose workhorse that may be leveraged to convert individual level records into aggregate information that may be more useful for some forms of epidemic modeling such as compartment modeling.

Up to this point, we have used **EpiCompare** in the context of observed data. We also want to compare statistical models, and **EpiCompare** aids in that process via a simple but dynamic individual-level data generator, conversion tools for popular epidemic model packages, and model assessments. We demonstrate an example here.

We first try to model the Hagelloch data with a stochastic SIR model, which we refer to as the ‘simple SIR.’ In our vignette, we show how to fit this simple SIR model via maximum likelihood and simulate from the model with those best fit parameters. Our function `simulate_agents()` generates individual level data according to discrete time multinomial draws, which depend on the number of individuals in each state at the previous time step and a matrix of transition probabilities. For example, the below code generates 100 simulations of an outbreak of a disease with one initial infector in a population of $n = 188$ individuals.

```
R> trans_mat <- matrix(c("X0 * (1 - X1 * par1 / N)", "X0 * X1 * par1 / N", "0",
+                        "0", "X1 * (1 - par2)", "par2 * X1",
+                        "0", "0", "X2"), byrow = TRUE, nrow = 3)

R> set.seed(2020)
R>
R> best_params <- c("beta" = .36, "gamma" = .13)
R> ## This is the SIR representation
R>
R> rownames(trans_mat) <- c("S", "I", "R")
```

```

R> init_vals <- c(187, 1, 0)
R> par_vals <- c(par1 = best_params[1], par2 = best_params[2])
R> max_T <- 55
R> n_sims <- 100
R>
R> agents <- simulate_agents(trans_mat,
+                             init_vals,
+                             par_vals,
+                             max_T,
+                             n_sims,
+                             verbose = FALSE)

R> agg_model <- agents %>% group_by(sim) %>%
+   agents_to_aggregate(states = c(I, R)) %>%
+   mutate(Type = "Simple SIR")

```

The result of our simulation is the object `agents` which is a 18800×5 data frame, which details the time of entry into the S , I , and R states for a given simulation. Before we examine the results of this simple SIR model, we will also examine another, more sophisticated SIR model, this time from the package **EpiModel**. Briefly, this model first fits a contact network to the set of individuals, where the class of the student is a covariate. The model then simulates a SIR-epidemic on that network.

```

R> library(EpiModel)
R> ## WARNING: Will take a minute or two
R>
R> set.seed(42)
R> nw <- network.initialize(n = 188, directed = FALSE)
R> nw <- set.vertex.attribute(nw, "group", rep(0:2, each = 90, 30, 68))
R> formation <- ~edges + nodematch("group") + concurrent
R> target.stats <- c(200, 300, 200)
R> coef.diss <- dissolution_coefs(dissolution = ~offset(edges), duration = 5)
R> est1 <- netest(nw, formation, target.stats, coef.diss, edapprox = TRUE)
R>
R> param <- param.net(inf.prob = 0.1, act.rate = 5, rec.rate = 0.1)
R> status.vector <- c(rep(0, 90), rep(0, 30), rep(0, 67), 1)
R> status.vector <- ifelse(status.vector == 1, "i", "s")
R> init <- init.net(status.vector = status.vector)
R> control <- control.net(type = "SIR", nsteps = 55,
+                         nsims = 100, epi.by = "group")
R> epimodel_sir <- netsim(est1, param, init, control)

```

The output of this model is `epimodel_sir`, an object of class `netsim`, which contains a plethora of modeling information. We provide the function `fortify_aggregate()`, which can take objects from specialized classes of modeling output and transform it into a tidy-style data frame.

```
R> fortified_net <- fortify_aggregate(epimodel_sir,
+                                   states = c("s.num", "i.num", "r.num")) %>%
+   mutate(Type = "EpiModel SIR",
+          sim = as.numeric(gsub("sim", "", sim)))
```

We can then analyze the results of the two models side by side as time-invariant epidemic curves. The results are shown in Figure 8, where a 90% prediction band is estimated from the delta ball method for each of the two models. For the Simple SIR model, we see that the data generally covers the data fairly well but clearly misses the second peak of infection. We also see that the prediction band is very large, covering up a large area of the ternary plot. On the other hand, for the **EpiModel** model, we see that the prediction band covers the data quite well and takes up less area.

```
R> both_models <- bind_rows(agg_model, fortified_net)
R>
R>
R> g <- ggplot() + geom_prediction_band(data = both_models %>% filter(t != 0),
+   aes(x = X0, y = X1, z = X2,
+       sim_group = sim, fill = Type),
+   alpha = .5,
+   conf_level = .90)
```

```
R> g +   geom_path(data = both_models %>% filter(t !=0),
+   aes(x = X0, y = X1, z = X2, group = paste(Type, sim)),
+   alpha = .3, col = "gray40") +
+   coord_tern() + theme_sir(base_size = 24) +
+   geom_point(data = hagelloch_sir,
+   aes(x = S, y = I, z = R), col = "black") +
+   labs(title = "Simple SIR model",
+   subtitle = "90% Prediction band and original data",
+   x = "S", y = "I", z = "R") +
+   scale_fill_manual(values = c("#006677", "#AA6600")) +
+   facet_wrap(~Type) +
+   theme(legend.position = "bottom")
```

Simple SIR model

90% Prediction band and original data

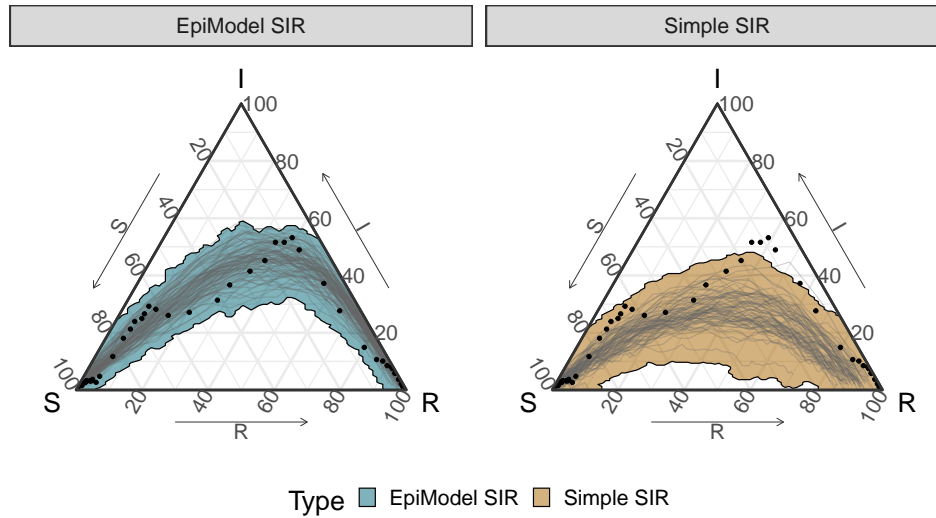


Figure 8: Original Hagelloch SIR data (black) along with 90% prediction band and actual simulation paths from the Simple SIR and the EpiModel SIR models.

However, both models are not a good fit to the filamental path as opposed to the individual points in (S, I, R) -space. This can be captured with the set of simulations both models predict, which all generally have a single defined peak of infection whereas the data certainly looks like it has two distinct peaks, likely caused by our assumed super-spreader event. This observation is backed up by the below analysis that demonstrates that the estimated pseudo-density of the observed epidemic (relative to the simulations from either model) is much less likely than **any** of the simulations (reported in Table 4). In conclusion, **EpiCompare** makes it clear that, at a glance, 1) the EpiModel network model is a better fit than the Simple SIR model, and 2) the fit is only good at the individual point level as opposed to the epidemic path level.

```
R> #-- after cleaning up and combining --
R> all_together_df <- rbind(simple_sir,
+                           hagelloch_sir2)
```

Table 3: Top and bottom 2 rows of `all_together_df`, combining both simulated epidemics and the true observation

Type	sim	t	S	I	R
Simple SIR	1	0	188	0	0
Simple SIR	1	1	187	1	0
true observation	0	54	1	0	187
true observation	0	55	1	0	187

```
R> compression_df <- all_together_df %>% group_by(Type, sim) %>%
+   filament_compression(data_columns = c("S", "I", "R"),
+   number_points = 20)
```

```

R> tdmat <- compression_df %>%
+   dist_matrix_innersq_direction(
+     position = c(1:length(compression_df))[
+       names(compression_df) %in% c("S", "I", "R")],
+     tdm_out = T)
R>
R> simple_sir_true_obs_info <- tdmat %>%
+   compare_new_to_rest_via_distance(
+     new_name_id = data.frame(Type = "true observation", sim = 0),
+     distance_func = distance_psuedo_density_function,
+     sigma = "20%")

```

Table 4: The extremeness of the true simulations based on comparing psuedo-density estimates between true vs simulated curves

Type	simulations-based estimated psuedo-density	proportion of simulations with lower estimated psuedo-density
Simple SIR	0.0036733	0
EpiModel SIR	0.0028813	0

A. Appendix

A.1 Proof of Theorem 1

Proof. [Harko et al. \(2014\)](#) provide an analytical solution for the Kermack and McKendrick equations (Eq. (1)) by reparameterizing the ODEs so that $\mathcal{S}(u) = S(t)$, $\mathcal{I}(u) = S(t)$, and $\mathcal{R}(u) = R(t)$ for $0 < u_T < 1$ with

$$\mathcal{S}(u) = S(0)u \tag{2}$$

$$\mathcal{I}(u) = N - R(0) + NR_0^{-1} \log u - S(0)u$$

$$\mathcal{R}(u) = R(0) - NR_0^{-1} \log u,$$

and u and t are related by the following integral,

$$\begin{aligned}
t &= \int_u^1 \frac{N}{\beta \tau (N - R(0) + R_0^{-1} \log \tau - S(0)\tau)} d\tau \\
&= \int_u^1 \frac{1}{\beta f(S(0), R(0), N, R_0, \tau)} d\tau \\
&= \int_u^1 \frac{1}{\beta f(\tau)} d\tau,
\end{aligned}$$

where we have made the denominator of the integral a function of N , the initial values, R_0 , and τ , which we further condense to $f(\tau)$ for brevity. Then for a given t we want to find s

such that $(S_1(t), I_1(t), R_1(t)) = (S_2(s), I_2(s), R_2(s))$. Or equivalently, for a fixed u want to find v such that $\mathcal{S}_1(u) = \mathcal{S}_2(v)$ and then the corresponding t and s are given by

$$\begin{aligned} t &= \int_u^1 \frac{1}{\beta_1 f(\tau)} d\tau \\ s &= \int_v^1 \frac{1}{\beta_2 f(\tau)} d\tau. \end{aligned}$$

Note that since the equations in Eq. (2) are functions of the initial values and R_0 , then $u = v$. We then can find a relation for s ,

$$\begin{aligned} s &= \int_u^1 \frac{1}{\beta_2 f(\tau)} d\tau \\ &= \int_u^1 \frac{1}{a\beta_1 f(\tau)} d\tau \\ &= \frac{1}{a} \int_u^1 \frac{1}{\beta_1 f(\tau)} d\tau \\ &= \frac{1}{a} t. \end{aligned}$$

□

References

- Anderson RM, May RM (1992). *Infectious diseases of humans: dynamics and control*. Oxford university press.
- Becker AD, Birger RB, Teillant A, Gastanaduy PA, Wallace GS, Grenfell BT (2016). “Estimating enhanced prevaccination measles transmission hotspots in the context of cross-scale dynamics.” *Proceedings of the National Academy of Sciences*, **113**(51), 14595–14600.
- Biggerstaff M, Alper D, Dredze M, Fox S, Fung ICH, Hickmann KS, Lewis B, Rosenfeld R, Shaman J, Tsou MH, Velardi P, Vespignani A, Finelli L, Chandra P, Kaup H, Krishnan R, Madhavan S, Markar A, Pashley B, Paul M, Meyers LA, Eggo R, Henderson J, Ramakrishnan A, Scott J, Singh B, Srinivasan R, Bakach I, Hao Y, Schaible BJ, Sexton JK, Del Valle SY, Deshpande A, Fairchild G, Generous N, Friedhorsky R, Hickman KS, Hyman JM, Brooks L, Farrow D, Hyun S, Tibshirani RJ, Yang W, Allen C, Aslam A, Nagel A, Stilo G, Basagni S, Zhang Q, Perra N, Chakraborty P, Butler P, Khadivi P, Ramakrishnan N, Chen J, Barrett C, Bisset K, Eubank S, Anil Kumar VS, Laskowski K, Lum K, Marathe M, Aman S, Brownstein JS, Goldstein E, Lipsitch M, Mekaru SR, Nsoesie EO, Gesualdo F, Tozzi AE, Broniatowski D, Karspeck A, Tse ZTH, Ying Y, Gambhir M, Scarpino S (2016). “Results from the centers for disease control and prevention’s predict the 2013-2014 Influenza Season Challenge.” *BMC Infectious Diseases*, **16**(1), 1–10. ISSN 14712334. doi: [10.1186/s12879-016-1669-x](https://doi.org/10.1186/s12879-016-1669-x). URL <http://dx.doi.org/10.1186/s12879-016-1669-x>.
- Britton T, Kypraios T, O’Neill PD (2011). “Inference for epidemics with three levels of mixing: methodology and application to a measles outbreak.” *Scandinavian Journal of Statistics*, **38**(3), 578–599.

- CDC (2021). “CDC COVID Data Tracker.” URL https://covid.cdc.gov/covid-data-tracker/#cases_casesper100klast7days.
- Ciollaro M, Genovese CR, Wang D (2016). “Nonparametric clustering of functional data using pseudo-densities.” *Electronic Journal of Statistics*, **10**(2), 2922–2972. ISSN 19357524. doi: [10.1214/16-EJS1198](https://doi.org/10.1214/16-EJS1198).
- Dong E, Du H, Gardner L (2020). “An interactive web-based dashboard to track COVID-19 in real time.” *The Lancet infectious diseases*, **20**(5), 533–534.
- Ferguson N, Laydon D, Nedjati Gilani G, Imai N, Ainslie K, Baguelin M, Bhatia S, Boonyasiri A, Cucunuba Perez Z, Cuomo-Dannenburg G, *et al.* (2020). “Report 9: Impact of non-pharmaceutical interventions (NPIs) to reduce COVID19 mortality and healthcare demand.”
- Gallagher S, Chang A, Eddy WF (2020). “Exploring the nuances of R0: Eight estimates and application to 2009 pandemic influenza.” *arXiv preprint arXiv:2003.10442*.
- Geenens G, Nieto-Reyes A (2017). “On the functional distance-based depth.”
- Groendyke C, Welch D, Hunter DR (2012). “A network-based analysis of the 1861 Hagelloch measles data.” *Biometrics*, **68**(3), 755–765.
- Hamilton NE, Ferry M (2018). “ggtern: Ternary Diagrams Using ggplot2.” *Journal of Statistical Software, Code Snippets*, **87**(3), 1–17. doi: [10.18637/jss.v087.c03](https://doi.org/10.18637/jss.v087.c03).
- Harko T, Lobo FS, Mak MK (2014). “Exact analytical solutions of the Susceptible-Infected-Recovered (SIR) epidemic model and of the SIR model with equal death and birth rates.” *Applied Mathematics and Computation*, **236**, 184–194. ISSN 00963003. doi: [10.1016/j.amc.2014.03.030](https://doi.org/10.1016/j.amc.2014.03.030). 1403.2160, URL <http://dx.doi.org/10.1016/j.amc.2014.03.030>.
- Jenness SM, Goodreau SM, Morris M (2018). “EpiModel: An R Package for Mathematical Modeling of Infectious Disease over Networks.” *Journal of Statistical Software*. doi: [10.18637/jss.v084.i08.EpiModel](https://doi.org/10.18637/jss.v084.i08.EpiModel).
- Kermack WO, McKendrick AG (1927). “A contribution to the mathematical theory of epidemics.” *Proceedings of the royal society of london. Series A, Containing papers of a mathematical and physical character*, **115**(772), 700–721.
- King AA, Nguyen D, Ionides EL (2016). “Statistical inference for partially observed markov processes via the R package pomp.” *Journal of Statistical Software*, **69**(12), 1–43. ISSN 15487660. doi: [10.18637/jss.v069.i12](https://doi.org/10.18637/jss.v069.i12). 1509.00503.
- Meyer S, Held L, Höhle M (2017). “Spatio-Temporal Analysis of Epidemic Phenomena Using the R Package surveillance.” *Journal of Statistical Software*, **77**(11), 1–55. doi: [10.18637/jss.v077.i11](https://doi.org/10.18637/jss.v077.i11).
- MIDAS Network (2021). “Online Portal for COVID-19 Modeling and Research.” URL <https://midasnetwork.us/covid-19/>.
- Neal PJ, Roberts GO (2004). “Statistical inference and model selection for the 1861 Hagelloch measles epidemic.” *Biostatistics*, **5**(2), 249–261. ISSN 14654644. doi: [10.1093/biostatistics/5.2.249](https://doi.org/10.1093/biostatistics/5.2.249).

Oesterle H (1992). “Statistische Reanalyse einer Masernepidemie 1861 in Hagelloch.”

Pfeilsticker A (1863). “Beiträge zur Pathologie der Masern mit besonderer Berücksichtigung der statistischen Verhältnisse.” URL <http://www.archive.org/details/beitrgezurpatho00pfeigoog>.

Rvachev LA, Longini IM (1985). “A mathematical model for the global spread of influenza.” *Mathematical Biosciences*, **75**(1), 3 – 22. ISSN 0025-5564. doi:[http://dx.doi.org/10.1016/0025-5564\(85\)90064-1](http://dx.doi.org/10.1016/0025-5564(85)90064-1). URL <http://www.sciencedirect.com/science/article/pii/0025556485900641>.

The Washington Post (2021). “Coronavirus US Cases and.” URL <https://washingtonpost.com/graphics/2020/national/coronavirus-us-cases-deaths/>.

Wickham H (2016). *ggplot2: Elegant Graphics for Data Analysis*. Springer-Verlag New York. ISBN 978-3-319-24277-4. URL <https://ggplot2.tidyverse.org>.

Wickham H, Averick M, Bryan J, Chang W, McGowan LD, François R, Golemund G, Hayes A, Henry L, Hester J, Kuhn M, Pedersen TL, Miller E, Bache SM, Müller K, Ooms J, Robinson D, Seidel DP, Spinu V, Takahashi K, Vaughan D, Wilke C, Woo K, Yutani H (2019). “Welcome to the tidyverse.” *Journal of Open Source Software*, **4**(43), 1686. doi: [10.21105/joss.01686](https://doi.org/10.21105/joss.01686).

Worby CJ, Chaves SS, Wallinga J, Lipsitch M, Finelli L, Goldstein E (2015). “On the relative role of different age groups in influenza epidemics.” *Epidemics*, **13**, 10–16.

Affiliation:

Shannon K. Gallagher
Biostatistics Research Branch
National Institute of Allergy
and Infectious Diseases
5603 Fishers Lane
Rockville, MD 20852
E-mail: shannon.gallagher@nih.gov
URL: <http://skgallagher.github.io>

Benjamin LeRoy
Dept. of Statistics & Data Science
Carnegie Mellon University
5000 Forbes Ave.
Pittsburgh, PA 15213
E-mail: bpleroy@andrew.cmu.edu
URL: <https://benjaminleroy.github.io/>